The patellazoles inhibit protein synthesis at nanomolar concentrations in human colon tumor cells

Adam D. Richardson[a], William Aalbersberg[b] and Chris M. Ireland[a]

The patellazoles are a family of compounds consisting of a 24-member macrolide ring with a thiazole-epoxide tail. The opening of this epoxide does not greatly affect the bioactivity of these compounds, although the cellular toxicity is generally decreased. The patellazoles are extremely cytotoxic towards HCT 116 human colon tumor cells. Treatment with nanomolar amounts of these compounds results in immediate inhibition of protein synthesis and cell cycle arrest at the G_1 and S phase. HCT 116 wild-type cells underwent apoptosis after extended patellazole treatment. Although treatment with the patellazoles resulted in an increased amount of p53, the p53 null cells were still strongly affected by treatment. The inhibition of translation by patellazole treatment is linked to the inhibition of the mTOR/p70 pathway. Like the mTOR inhibitor rapamycin, the patellazoles inhibit translation through the 4EBP1 and S6 kinase pathways. However, the cytotoxicity of rapamycin and the patellazoles differs greatly in HCT 116 cells. The cellular target of the patellazoles is still unknown; the patellazole-induced inhibition of this pathway occurs either downstream or parallel to AKT. *Anti-Cancer Drugs* **16:533–541 © 2005 Lippincott Williams & Wilkins.**

Anti-Cancer Drugs 2005, **16**:533–541

Keywords: patellazole, rapamycin, colon tumor, cytotoxicity, cell cycle arrest, translation, mTOR

[a]Department of Medicinal Chemistry, University of Utah, Salt Lake City, UT, USA and [b]Institute of Applied Sciences, University of the South Pacific, Suva, Fiji.

Sponsorship: A. D. R. has been supported by fellowships from the American Foundation for Pharmaceutical Education and the American Chemical Society Division of Medicinal Chemistry. This project was funded by NIH grant CA36622.

Correspondence to C. M. Ireland, Department of Medicinal Chemistry, University of Utah, Salt Lake City, UT 84112, USA.
Tel: +1 801 581-8305; fax: +1 801 585-6208;
e-mail: cireland@pharm.utah.edu

Received 9 September 2004 **Revised** form accepted 9 February 2005

Introduction

The patellazoles are a family of marine natural products which contain a 24-member macrolide ring and a thiazole-containing tail. These compounds, shown in Figure 1, were first described in 1988 in concurrent papers by Zabriskie *et al.* [1] and Corley *et al.* [2]. The ascidian *Lissoclinum patella* was collected in Fiji by the Ireland group and in Guam by the Paul group. To date, only *L. patella* collected in Fiji and Guam has yielded any patellazoles. Investigations of *L. patella* collected in the Philippines, Australia and Indonesia have so far failed to yield the patellazoles. Zabriskie and Ireland provided the structure elucidation of patellazoles A–C, while Corley and Paul described patellazole B. Additionally, Zabriskie partially described another four members of the patellazole family (patellazoles D–G) [3].

The patellazoles are extremely cytotoxic, particularly patellazole B, but neither the mechanism of action nor the cellular target of these compounds is known. Some interesting data have been identified, however. The mean IC_{50} of patellazoles A, B and C against the NCI human cell line panel was 3×10^{-4}, $< 10^{-6}$ and 3×10^{-3} μg/ml, respectively [3]. Similar values were reported for these compounds against the L1210 murine leukemia cell line. Patellazole B was also reported to be 20 times more toxic in p21-deficient cells than in the parental wild-type cell line [3].

Interestingly, treatment with the patellazoles causes an increase in DNA synthesis [3], but the patellazoles do not interact with DNA or any topoisomerase (unpublished result). An increase in DNA synthesis is often the result of DNA damage; however, this does not seem to be the case with the patellazoles. Additionally, patellazoles B and C were found to have excellent antiviral activity against herpes simplex viruses 1 and 2 *in vitro*, but not *in vivo* [3].

Due to these interesting biological properties, we wished to re-isolate patellazoles A–C for use in pharmacologic studies. This re-isolation was not without difficulty, however. The initial attempt in 1998 yielded not patellazoles A–C, but very small amounts of new patellazoles instead [4]. These patellazole analogs are named patellazoles H–J and are shown in Figure 2. During the isolation process it appears that the epoxide present in the natural products was opened by the addition of either methanol or isopropanol at carbon 31. A re-collection of *L. patella* from Navula Pass, Fiji, in October of 2001 did yield significant amounts of patellazoles A–C. The combination of the minute

0959-4973 © 2005 Lippincott Williams & Wilkins

Copyright © Lippincott Williams & Wilkins. Unauthorized reproduction of this article is prohibited.

Fig. 1

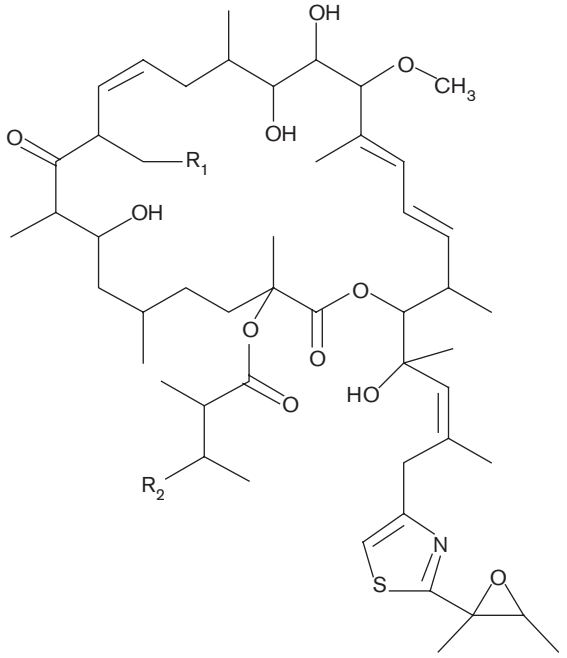

Patellazoles A–C. A: $R_1 = R_2 = H$; B: $R_1 = H$, $R_2 = OH$; C: $R_1 = R_2 = OH$.

Fig. 2

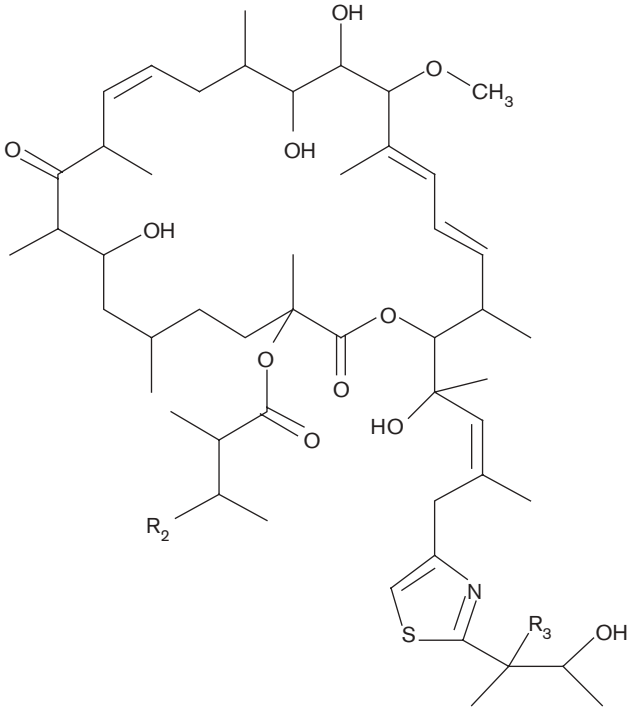

Patellazoles H–J. H: $R_2 = OH$, $R_3 = OCH_3$; I: $R_2 = H$, $R_3 = OCH_3$; J: $R_2 = OH$, $R_3 = OCH(CH_3)_2$.

amounts of patellazoles H–J available and the initial lack of patellazoles A–C is the reason why some of the experiments described in this report use only certain patellazoles and not others. Fortunately, the only difference in biological activity between the various patellazoles appears to be potency, while the overall mechanism of action remains the same.

Materials and methods

All materials used in cell culture, including media components, disposable cultureware and major equipment, were purchased from Fisher Scientific (Denver, CO) unless otherwise noted. Molecular biology tools, except for antibodies, were purchased from Invitrogen (Carlsbad, CA) unless noted.

L. patella, 200 g dry weight, was collected in the Fiji Islands near Kadavu by SCUBA in 1997 and frozen until used. Purification began with extraction, solvent partitioning and silica flash chromatography. The early eluting fractions were subjected to silica HPLC using a Whatman Partisil Magnum 9 (10×500 mm and 10 μm particle size) silica column (Clifton, NJ). The solvent system was a gradient from 95:5 hexane: isopropanol to 70:30 hexane:isopropanol with a flow rate of 5 ml/min. The purification yielded only 1.7 mg of patellazole H, 0.00085% yield (w/w), 0.7 mg of patellazole I, 0.00035% yield (w/w) and 0.6 mg of patellazole J, 0.0003% yield (w/w) [4].

L. patella yielding patellazole A–C was collected in the Fiji Islands from Navula Pass in October of 2001. Following extraction and solvent partitioning, the chloroform fraction was separated using a silica flash column as above. The fraction eluted with 9:1 EtOAc:MeOH contained 158.6 mg of mixed patellazoles A and B. The front of the methanol wash contained 230.3 mg crude patellazole C. The crude patellazole C was eluted using a C_{18} column (1.5×200 cm) in a 9:1 methanol:water solvent system yielding 190.0 mg pure patellazole C (0.14%, w/w). The fraction containing patellazoles A and B was separated and purified using a Phenomenex diol column (250×10 mm, 5 μm particle) and an isocratic 60:40 hexane:chloroform solvent system at 3 ml/min solvent flow, yielding 27.8 mg patellazole A (0.02%, w/w) and 40.0 mg patellazole B (0.03%, w/w).

Tissue culture

All cell cultures were grown at 37°C, 5% CO_2 and maximal humidity (by equilibration). All media reagents were purchased from Invitrogen (Carlsbad, CA). The HCT 116 strains were generously donated by Dr Bert Vogelstein (Johns Hopkins University), and grown in McCoy's 5A media supplemented with 10% v/v heat-inactivated FBS, 1% v/v MEM sodium pyruvate, 1% v/v penicillin/streptomycin and 1% v/v L-glutamine. Caco2,

Copyright © Lippincott Williams & Wilkins. Unauthorized reproduction of this article is prohibited.

MDA MB-435S and MDA MB-468 cell lines were purchased from the ATCC (Manassas, VA). Cells were counted using a Beckman (Fullerton, CA) Coulter cell counter.

Cytotoxicity

The ability of the patellazoles to inhibit cellular growth was determined using an MTT assay. An appropriate number of cells (based upon cell type) was plated in 96-well plates in 200 µl of media and the cells were allowed to grow overnight. Serial dilutions of patellazoles were then added to the wells in quadruplicate. Control wells were treated with vehicle dimethylsulfoxide (DMSO). After 72 h of incubation the media were removed and 100 µl fresh media added along with 10 µl of MTT (Acros Organics, Denver, CO). The cells were then incubated for 4 h under the same conditions as above. The media were then removed and 100 µl DMSO added to each well. The amount of formazan resulting from MTT metabolism was measured by observing absorbance at 540 nm using a Labsystems Multiskan Plus plate reader. Using the absorbance in the vehicle-treated lanes as 0% growth inhibition, the amount of patellazole needed to cause a 50% inhibition in growth was determined.

Flow cytometry

In each experiment, 1.2×10^6 HCT 116 cells were plated in 2 ml of media in 25-cm^2 flasks and allowed to grow overnight. Each flask was then treated with patellazole or vehicle (DMSO) and incubated for either 24 or 48 h. The media were collected and the cells washed with 2 ml versene. The versene wash was pooled with the corresponding media and the cells incubated at room temperature for 5 min with 1 ml trypsin–EDTA. Trypsinization was quenched with 4 ml of media and the media-trypsin was pooled with the corresponding media-versene in 15 ml centrifuge tubes. Cells were collected by centrifugation at 305 *g* for 5 min. The supernatant was gently removed and the cell pellets were resuspended in cold phosphate-buffered saline (PBS) to a final concentration of $1–2 \times 10^6$ cells/ml. Ice-cold methanol was then slowly added dropwise with gentle vortexing to a volume of 2 times the volume of PBS. The fixed cells were stored at 4°C for between 24 and 72 h. The cells were then submitted to the University of Utah Flow Cytometry Resource Facility for propidium iodine staining and FACS analysis. The data presented here are representative of multiple experiments; most doses/times were repeated at least 3 times.

Protein isolation

Using six-well plates, 4×10^5 HCT 116 cells were plated per well in 2 ml media, and allowed to attach and grow overnight. Each well was then treated with drug and incubated for either 24 or 48 h. The plates were then placed on ice and media removed. The cells were washed twice with 1 ml ice-cold PBS and incubated on ice for 10 min with 200 µl lysis buffer (25 mM Tris, pH 7.4, 150 nM NaCl, 1 mM $CaCl_2$, 1% Triton-X, 10 ng/ml leupeptin, 10 ng/ml aprotinin, 1 mM phenylmethylsulfonyl fluoride, 53.3 mM NaF and 2 mM Na_3VO_4). [Due to their instability in solution, the leupeptin, aprotinin, phenylmethylsulfonyl fluoride and Na_3VO_4 were added immediately prior to use.] The cells were then disrupted by vigorous scraping and the lysate centrifuged at 4°C for 10 min. The supernatant was gently removed and the debris pellet was discarded. The amount of protein per lysate solution was quantified using the DC Protein Assay from Bio-Rad (Hercules, CA) [5]. The lysates were stored at −70°C until used.

Western blotting

All gels, molecular weight markers, electrophoresis and transfer buffers were purchased from Invitrogen (Carlsbad, CA). All antibodies were purchased from Cell Signaling Technologies (Beverly, MA) except for anti-poly(ADP-ribose) polymerase (PARP), which was purchased from PharMingen (Boston, MA). Polyvinylidene fluoride (PVDF) membranes were purchased from VWR (West Chester, PA). Luminol reagent was purchased from Santa Cruz Biotechnology (Santa Cruz, CA). NuPAGE 4–12% Bis–Tris gradient gels were used with NuPAGE MESI SDS running buffer and NuPAGE transfer buffer in all experiments and run according to manufacturer's instructions [6].

Samples were prepared with 10 µg protein (quantified as described above), 5 µl NuPAGE 4 × LDS sample buffer and 2 µl NuPAGE 10 times reducing agent and all sample volumes were normalized to 20 µl with purified water. Samples were heated to 70°C for 10 min and loaded onto the gel. Gels were electrophoresed at 200 V for 35–45 min and transferred to a PVDF membrane at 300 mA for 1 h.

The membrane was incubated for 1 h at room temperature or overnight at 4°C in freshly prepared blocking buffer (2 g non-fat dry milk in 50 ml PBS/0.1% Tween 20) with gentle agitation. The blocking buffer was removed, and the membrane rinsed twice with PBST and then incubated in the appropriate primary antibody dilution overnight at 4°C with gentle agitation. Primary antibodies were diluted to 1:1000 (v/v) in primary antibody solution [5% w/v bovine serum albumin (BSA) and 0.02% w/v sodium azide in PBST].

The primary antibody solution was removed and the membrane washed with PBST 3 times for 10 min each at room temperature. The membrane was incubated for 60 min in the appropriate horseradish peroxidase-conjugated secondary antibody (diluted 1:10,000 in freshly prepared blocking buffer). The membrane was then washed again with PBST 3 times for 10 min each and the protein–antibody conjugates detected by chemiluminescence. Equal loading of lanes was confirmed through

Copyright © Lippincott Williams & Wilkins. Unauthorized reproduction of this article is prohibited.

either the examination of non-specific bands or a second primary antibody probe; if no non-specific binding occurred the membrane was reprobed with ubiquitin as a loading control.

Macromolecular synthesis

[^{3}H]Thymidine, [^{3}H]uracil and [^{3}H]lysine were used to observe DNA, RNA and protein synthesis, respectively. Aqueous solutions of radiolabeled precursors (1.0 μCi/μl) were purchased from Perkin-Elmer (Boston, MA); optiphase 'SuperMix' scintillation fluid was purchased from Fisher Chemicals (Loughborough, UK); samples were counted using a Packard liquid scintillation analyzer, model 1900TR (Meriden, CT). A vacuum-filtering manifold, purchased from Hoefer Scientific Instruments (San Francisco, CA), was used for filtration and washing.

A pulse–chase experiment was performed in which HCT 116 wild-type cells were treated with either 30 nM patellazole H or DMSO (control) for 3, 18 or 30 h before being exposed to the tritium-labeled precursors. After 30 min of incubation with the radiolabeled precursors, fresh media were applied and the cells incubated for another 30 min to increase the amount of radiolabel incorporation. The cells were then lysed with a 0.1% SDS solution and the macromolecules precipitated using 50% perchloric acid. The precipitate was collected by vacuum filtration through Whatman GF/C grade glass-fiber filters and allowed to quench in scintillation fluid in the dark for 48 h. The amount of radioactivity (d.p.m.) for each precursor was then determined, and the amount of macromolecular synthesis compared for the treated and control cultures.

DNA microarray

mRNA was isolated from both drug-treated and non-treated (control) cells. Reverse transcriptase and labeled nucleotide analogs were used to prepare differentially tagged cDNA from each mRNA [Cy3-dCTP (green fluorescence) and Cy5-dCTP (red fluorescence)]. The tagged cDNA species were mixed in equal amounts and hybridized to a slide spotted with thousands of genes. The slides were prepared by the Microarray Core Facility at the Huntsman Cancer Institute (University of Utah). Each slide harbors 4632 individual human cDNA clones in duplicate. A collection of 78 control samples are printed on each slide including positive and negative controls such as housekeeping genes, tissue-specific genes and non-human sequences to monitor the fluorescent labeling efficiency and non-specific cross-hybridization. The amount of each fluorescent tag hybridized to each gene spot was detected using a two-color confocal laser microscope and ImageQuant NT software. If treatment with the drug caused differential transcription of a particular gene, this may be observed as the predominance of one type of fluorescence [7,8].

Total RNA isolation

Total RNA was isolated using TRIzol LS Reagent purchased from Life Technologies (Carlsbad, CA). The manufacturer's protocol was generally followed [9]. Diethyl pyrocarbonate (DEPC) was purchased from Sigma-Aldrich (St Louis, MO). All other chemicals and RNase-free polypropylene flasks were purchased from Fisher Scientific. RNase-free water was prepared by adding DEPC to purified water (0.01% v/v) in RNase-free glass bottles and then autoclaved.

In the experiment, 1.2×10^6 HCT 116 cells were plated in 15 ml of media in 75-cm^2 flasks and allowed to grow overnight at 37°C. HCT 116 wild-type cells were treated with either 27.9 nM patellazole B or the identical volume of DMSO for 18 h. At that time, the media were removed and 10 ml TRIzol solution added to each flask. Flasks were incubated at room temperature for 5–7 min and the solution then transferred to 15-ml polypropylene conical tubes. Chloroform (3 ml) was added to each of the tubes, mixed by inverting several times and incubated at room temperature for 2 min. The tubes were then centrifuged at 3200 *g* and 4°C for 45–60 min. The upper (aqueous) phase, about 6 ml, was transferred to a fresh 15 ml polypropylene conical tube. An equal volume of isopropanol was added to each tube. Precipitate was allowed to form at room temperature for 10 min, at which time the flasks were centrifuged at 3200 *g* and 4°C for 45–60 min. The supernatant was removed and the pellets transferred to 2 ml microcentrifuge tubes where they were washed with 400 μl 80% ethanol. These were centrifuged again at 7000 *g* and room temperature for 5 min to reform pellet. The supernatant was removed and the pellet dried at room temperature for 10 min. The pellet was resuspended in 200 μl DEPC H_2O by gently vortexing. The concentration of RNA was determined by the A_{260}/A_{280} absorbance ratio using a Beckman model DU-530 spectrophotometer.

mRNA isolation

The PolyATract mRNA Isolation System III (Promega, Madison, WI) was used to isolate mRNA from the total cellular RNA. The manufacturer's protocol was generally followed [10]. The total RNA samples were brought to a final volume of 500 μl by adding DEPC H_2O and heated to 65°C for 10 min. The biotinylated oligo(dT) probe was annealed to the mRNA by adding 3 μl of the probe and 13 μl of 20 × SSC buffer (3 M NaCl and 0.3 M sodium citrate) to each sample. The samples were gently vortexed and allowed to cool for 10 min. Streptavidin-bound paramagnetic spheres [poly(A)] were added to bind biotinylated oligo(dT) and magnetically separated, then resuspended and washed 3 × 300 μl with 0.5 × SSC buffer and resuspended in 100 μl of the same buffer. This was done twice and the washes pooled. The concentration and purity of the mRNA solution was determined spectrophotometrically by measuring the A_{260}/A_{280}

Copyright © Lippincott Williams & Wilkins. Unauthorized reproduction of this article is prohibited.

absorbance ratio, which was 1.7–1.9 for all samples. Samples were immediately frozen to –70°C and submitted to the Microarray Core Facility at the Huntsman Cancer Institute, University of Utah.

Results

The ability of both the natural products and the solvent–adduct analogs to inhibit cellular growth was examined in HCT 116 cell lines using the MTT assay. This assay measures the amount of total growth inhibition through observing the activity of cellular mitochondria [11]. The patellazoles are very potent inhibitors of cellular growth, as shown in Table 1.

Patellazole B has been previously reported as the most cytotoxic of the three patellazole natural products [3]. Analyzing the relative cytotoxicity of the natural products and the analogs resulted in an interesting pattern, as shown in Figure 3. Patellazoles A and B were found to be similarly cytotoxic, with patellazole B displaying greater toxicity in some cases. Patellazole J, the isopropanol adduct of patellazole B, showed the next greatest cytotoxicity, followed by patellazole C, I and H. Patellazole J is approximately an order of magnitude less cytotoxic than the natural product it was derived from. Patellazole H, the addition of methanol to patellazole B, is approximately two orders of magnitude less cytotoxic than its parent natural product. The addition of methanol to patellazole A, creating patellazole I, causes an order of magnitude loss of cytotoxicity.

The cleavage of PARP from a native 116-kDa form to 85- and 31-kDa fragments is an early event during caspase-mediated apoptosis [12]. Treatment of HCT 116 wild-type cells with 30 nM patellazole H for 18 h caused PARP cleavage indicating that apoptotic pathways had been activated. This Western blot is shown in Figure 4.

Table 1 **IC_{50} values for the patellazoles in three HCT 116 cell lines (nM)[a]**

Patellazole	HCT 116 wild-type	HCT 116 $p53^{-/-}$	HCT 116 $p21^{-/-}$
A	0.62	0.66	–[b]
B	0.39	0.62	–[b]
C	4.70	5.60	–[b]
H	30.0	34.0	9.0
I	8.80	8.30	2.4
J	2.60	3.00	1.0

[a]72 h incubation time.
[b]Not tested.

Fig. 3

B > A > J > C > I > H
(B + IPA) (A + MeOH) (B + MeOH)

Relative cytotoxicities of the patellazoles toward the HCT 116 wild-type cell line. Patellazole B is the most cytotoxic, patellazole H the least. The parent natural product and solvent adduct is listed below each of the artifacts.

Fig. 4

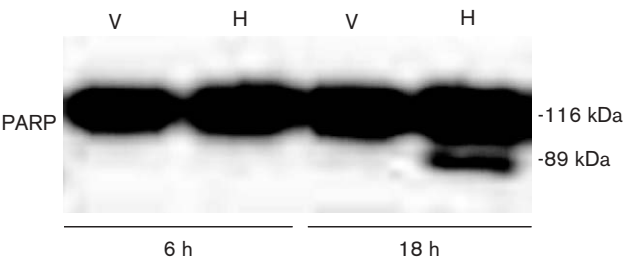

The effect of patellazole H on PARP. Treatment with an IC_{50} value of patellazole H (H) after 6 h or 18 h as compared to the vehicle-treated control (V).

Table 2 **Fractional survival of various cell lines when treated with 1 μg/ml[a] of patellazoles[b]**

Patellazole	Caco2	MDA-MB-435S	MDA-MB-468
A	0.86	0.72	0.62
B	0.89	0.92	0.87
C	0.74	0.79	1.10
H	0.85	0.83	0.71
I	0.83	0.56	0.46
J	0.72	0.77	1.01

[a]Approximately 1.1 μM each.
[b]72 h incubation time.

The ability of the patellazoles to inhibit the growth of Caco2 cells (a colon tumor cell line that is able to differentiate) and two breast cancer cell lines is shown in Table 2. This data is presented at percent inhibition as the IC_{50} values were too large to be determined (due to supply and solubility limitations). The two breast cancer cells lines are MDA-MB-435S (which over expresses epidermal growth factor receptor) and a daughter cell line, MDA-MB-468, in which both copies of PTEN have been disrupted. Surprisingly, none of the patellazoles showed significant cytotoxicity toward these cell lines, although another compound isolated from this organism, lissoclinolide, displayed similar toxicity toward both the HCT 116 cell lines, and the Caco2 and MDA-MB cell lines [13].

Patellazoles A–C and H–J all have the ability to arrest cells in the G_0/G_1 or S phase of the cell cycle. As shown in Table 3, treatment of wild-type HCT 116 cells with the IC_{50} concentration of each patellazole artifact resulted in an increase in the percentage of cells in G_0/G_1 after 24 h of exposure. The amount of cellular debris increased as compared to the control, indicating that these patellazoles were inducing cell death. At this time point,

Copyright © Lippincott Williams & Wilkins. Unauthorized reproduction of this article is prohibited.

Table 3 Cell cycle effect of IC_{50} concentrations of patellazoles on HCT 116 wild-type cells

Treatment	Duration (h)	G_0/G_1	S	G_2/M	Debris
Control	24	48.81	33.87	17.32	1.95
Patellazole H	24	58.69	32.46	8.84	9.48
Patellazole I	24	57.13	33.93	8.94	7.44
Patellazole J	24	59.19	28.65	12.15	9.31
Control	48	76.87	13.92	9.21	7.83
Patellazole H	48	54.68	39.76	5.55	84.09

Table 4 Cell cycle effect of IC_{50} concentrations of patellazoles on HCT 116 wild-type cells

Treatment	Duration (h)	G_0/G_1	S	G_2/M	Debris
Control	24	50.1	34.5	15.4	4.0
Patellazole A	24	60.6	29.0	10.4	5.0
Patellazole B	24	67.7	25.3	7.0	4.9
Patellazole C	24	71.2	19.3	9.6	6.7
Control	48	68.0	25.9	6.2	7.8
Patellazole A	48	60.5	32.1	7.4	16.0
Patellazole B	48	69.8	24.7	5.5	21.5
Patellazole C	48	62.3	31.2	6.4	17.5

Table 5 Cell cycle effect of 30 nM patellazole on HCT 116 wild-type cells

Treatment	Duration (h)	G_0/G_1	S	G_2/M	Debris
Control	24	42.6	41.5	15.9	23.5
Patellazole A	24	33.5	58.0	8.5	36.8
Patellazole B	24	33.4	57.2	9.4	31.4
Patellazole C	24	33.3	58.2	8.6	38.2
Control	48	70.0	24.0	5.9	18.1
Patellazole A	48	36.0	49.7	14.2	64.0
Patellazole B	48	40.3	47.8	12.0	66.8
Patellazole C	48	41.8	44.4	13.8	62.8

Table 6 Effect of 30 nM patellazole H on macromolecular precursor incorporation

Precursor	Treated/control ratio[a]		
	3 h	18 h	30 h
[^{3}H]Thymidine	1.02	2.80	1.22
[^{3}H]Uracil	1.14	0.61	0.23
[^{3}H]Lysine	0.65	0.31	0.13

[a]Values indicate relative incorporation in patellazole- versus vehicle-treated HCT 116 wild-type cells.

the percentage of cells in S phase did not increase. After 48 h of exposure to an IC_{50} concentration of patellazole H, the percentage of cells in G_0/G_1 decreased, while the percentage in S rose. However, the amount of cellular debris was also greatly increased. Most likely, cells that had been arrested in G_0/G_1 had either died, resulting in the large amount of cellular debris, or slowly progressed across the G_0/G_1 check point and rearrested in S phase.

The HCT 116 wild-type cells display a similar response to treatment with IC_{50} values of the patellazole natural products (Table 4). The percentage of cells in G_0/G_1 increases after 24 h of exposure to the drugs; after 48 h of exposure there is a decrease in G_0/G_1 arrested cells with a corresponding increase in the amount of cellular debris. Like patellazole H, the natural products also cause an increase in the percentage of cells in S phase at this time point.

Incubation of HCT 116 wild-type cells with 30 nM patellazoles A, B or C for 24 or 48 h all resulted in a decrease in the percentage of cells in G_0/G_1 as compared to the vehicle treated control (Table 5). This effect is particularly strong after a 48-h exposure. As observed in the IC_{50} experiments, this decrease in G_0/G_1 arrest cells correlates with an increase in cells arrested in S phase and in the amount of cellular debris. Apparently, as exposure time or dose of the patellazoles increases, HCT 116 wild-type cells transition from G_0/G_1 arrest to either S phase arrest or cell death.

The ability of patellazole H to inhibit the cellular synthesis of macromolecules was examined using radiolabeled precursors. A pulse–chase experiment was performed in which HCT 116 wild-type cells were treated with 30 nM patellazole H for 3, 18 or 30 h before being exposed to the tritium-labeled precursors. [^{3}H]Thymidine, [^{3}H]uracil and [^{3}H]lysine were used to observe DNA, RNA and protein synthesis, respectively. The level of radioactivity for each precursor was then determined, and the amount of macromolecular synthesis compared between the treated and control cultures. The results are shown in Table 6.

Protein synthesis began to decrease after only 3 h of exposure to 30 nM patellazole H (to 65% that of the control culture) and continued to decrease to 13% that of the control culture after 30 h of treatment. RNA synthesis also decreased, although not as rapidly. The first inhibition of RNA synthesis was observed after 18 h of exposure (61% that of the control culture) and continued to 30 h (23% that of the control culture). DNA synthesis increased dramatically after 18 h of treatment to 280% that of the control culture and then returned to near the control rate of synthesis after 30 h of exposure. It is not clear whether the amount of DNA synthesis would have continued to decrease to less than that of the control culture if a longer time point had been observed.

The effect of the patellazoles on protein synthesis was further illustrated by a DNA microarray experiment. In this experiment, HCT 116 wild-type cells were treated with either 27.9 nM patellazole B or DMSO (vehicle) for 18 h. mRNA was then isolated from both treated and control cells and the mRNA submitted to the Microarray Core Facility at the Huntsman Cancer Institute

Copyright © Lippincott Williams & Wilkins. Unauthorized reproduction of this article is prohibited.

(University of Utah). There were 74 genes for which a significant increase in transcription was observed. 'Significant' was defined at having an increase in transcription at least 2σ different from the mean of all gene changes. No genes were observed to be significantly downregulated by patellazole treatment in this experiment.

Twelve of the 74 genes observed to be upregulated after treatment of HCT 116 wild-type cells with 27.9 nM patellazole B encode ribosomal proteins (Table 7). This may be an attempt by the cells to compensate for the decrease in protein synthesis after patellazole treatment. Two other increasingly transcribed genes encode caspases involved in apoptosis. This, along with the observation of PARP cleavage after treatment and the accumulation of cell debris, illustrates the ability of the patellazoles to induce cell death. Of the remaining cDNA sequences observed to be up-regulated following patellazole treatment, approximately half were unknown ESTs at the time of this work and remain to be investigated.

Interestingly, treatment of HCT wild-type cells resulted in the upregulation of the rapamycin binding partner FK506-binding protein 1 (FKBP1) to levels 4.4 times that of the vehicle-treated cells. FKBP1 is the binding partner of the immunosuppressant rapamycin. Its activity is derived from its ability to inhibit translation, including the production of proteins required for cell cycle progression from G_1 to S phase. When rapamycin binds to FKBP1 the resultant complex directly inhibits mTOR. The inhibition of mTOR results in the inhibition of translation through 4EBP1 and p70. Additionally, a G_1 phase cell cycle arrest is mediated by the inhibition of cyclin-dependent kinase activation, the phosphorylation of retinoblastoma protein and a reduction in the amount of the protein cyclin D1 [14].

Table 7 Selected mRNA transcripts upregulated after treatment of HCT 116 wild-type cells with 27.9 nM patellazole B (versus vehicle treated)

Gene product	Expression ratio (treated/control)
60S ribosomal protein L13	5.31
60S ribosomal protein L6	5.60
60S ribosomal protein, large P2	5.67
60S ribosomal protein L32	6.16
60S ribosomal protein L11	6.23
60S ribosomal protein L13A	6.86
60S ribosomal protein L18A	7.39
60S ribosomal protein L8	7.49
40S ribosomal protein S5	4.44
40S ribosomal protein S19	4.84
40S ribosomal protein S9	5.69
40S ribosomal protein S23	6.06
Apoptotic cysteine protease Mch4	3.46
Apoptotic cysteine protease Mch2	4.32

However, HCT 116 cells were relatively resistant to rapamycin compared to the patellazoles. The IC_{50} of rapamycin was observed to be 10 μM in the HCT 116 wild-type cell line used here, as compared to the low nanomolar IC_{50} values for the patellazoles. The Western blots shown in Figures 5–7 utilized the IC_{50} value of both patellazole H and rapamycin; thus the cells were exposed to approximately 30 times more rapamycin than patellazole H.

Rapamycin is known to strongly inhibit the phosphorylation of p70 at threonine 389 [14]. This position is phosphorylated by mTOR. The phosphorylation of serine 421 is under the control of the mitogen-activated protein kinase (MAPK) pathway [15], which has not been previously described to be affected by rapamycin. However, the Western blot depicted in Figure 5 shows that rapamycin has the ability in HCT 116 wild-type cells to reduce the amount of phosphorylation at both Ser421 and Thr389. Patellazole H also inhibits the phosphorylation at Thr389, although less quickly than rapamycin. Patellazole H does not appear to affect the phosphorylation state of Ser421 (Fig. 5) nor does it effect the phosphorylation state of MAPK (data not shown).

The effect of both drugs is also observed downstream of p70. 4EBP1 is a regulatory protein that binds to eIF4E when not phosphorylated. When phosphorylated, the binding is disrupted and eIF4E associates with a large

Fig. 5

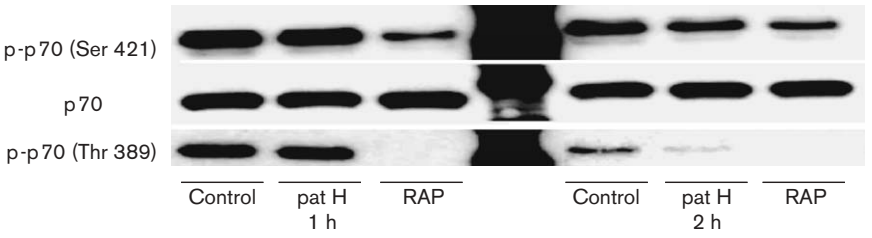

The effect of 30 nM patellazole H (pat H) or 10 μM rapamycin (RAP) versus DMSO (control) after either 1 or 2 h of exposure on the phosphorylation state and total expression of p70 after 1 or 2 h of exposure.

Copyright © Lippincott Williams & Wilkins. Unauthorized reproduction of this article is prohibited.

Fig. 6

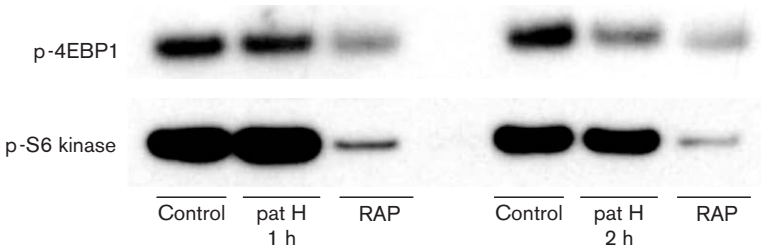

The effect of 30 nM patellazole H (pat H) and 10 μM rapamycin (RAP) versus DMSO (control) after either 1 or 2 h exposure on the phosphorylation state of 4EBP1 and S6 kinase.

Fig. 7

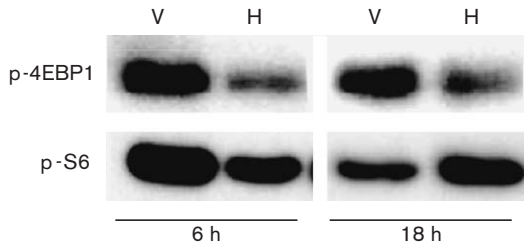

The effect of 30 nM patellazole H (H) versus DMSO (V) on the phosphorylation state of 4EBP1 and S6 kinase.

protein complex that initiates translation. Thus, the decrease in the phosphorylation of 4EBP1 causes a decrease in translation. Rapamycin inhibits this phosphorylation after 1 and 2 h of treatment; patellazole H begins to have an effect only after 2 h (Fig. 6).

Another branch of the p70 pathway involves the ribosomal protein S6 kinase. This protein also assists in protein translation but only when phosphorylated by p70. Rapamycin greatly inhibits this phosphorylation after 1 and 2 h of exposure, while patellazole H does not (Fig. 6).

However, after 6 h of exposure to patellazole H the phosphorylation of both 4EBP1 and S6 kinase are decreased (Fig. 7). Interestingly, the inhibition is sustained in 4EBP1 after 18 h of drug exposure while the phosphorylation of S6 kinase actually increases above that of the control levels. This may indicate that patellazole H preferentially affects one branch of the p70 pathway.

Discussion

The patellazoles are highly cytotoxic thiazole-containing macrolides with a range of bioactivity. The formation of patellazoles H–J from patellazoles A and B decreased cytotoxicity by either 10 or 100 times, depending upon the natural product and solvent involved. The two main possibilities for this pattern of altered cytotoxicity are (1) that the opening of the epoxide and resulting functional groups result in altered affinity for the patellazole target, or (2) the solvent addition changes either the ability of the compound to enter the cells or the distribution of the compound within the cells. Without further understanding the mechanism of action of the patellazoles or determining the cellular targets; it is not possible to determine the structure–activity relationships between these compounds. However, the opening of the epoxide by no means abrogates the cytotoxicity of the patellazoles, and the overall biological profile of the solvent-generated analogs and the natural products is very similar.

Three major responses to treatment with the patellazoles were identified. First, from a general cellular perspective, treatment with nanomolar concentration of the patellazoles resulted in the activation of apoptotic pathways and cell death. Second, both the natural products and the analogs had the ability to arrest HCT 116 cells in the G_0/G_1 phase of the cell cycle, followed by either an increase in the S phase population or apoptosis, depending upon treatment dose and duration. Third, patellazole treatment caused a sharp increase in DNA synthesis and a concurrent depression of protein synthesis.

Patellazoles H–J were used to examine whether the presence or absence of the cyclin-inhibiting protein p21 affected the ability of HCT 116 cells to respond to patellazole treatment. HCT 116 $p21^{-/-}$ cells were approximately 3 times more sensitive toward each of the three analogs than the parental p21-competent cell line. This is a typical response for a compound which causes G_0/G_1 or S phase arrest of the cell cycle. Although treatment with patellazoles resulted in arrest in the G_0/G_1 and S phases of the cell cycle, the cyclins E, B1 and D as well as CDKs 2 and 4 were not observed to be effected (data not shown).

Copyright © Lippincott Williams & Wilkins. Unauthorized reproduction of this article is prohibited.

The third major cellular response to the patellazoles is the effect on macromolecular synthesis. HCT 116 wild-type cells displayed increased DNA synthesis after treatment with patellazole H, as has been previously described [3]. RNA synthesis decreased over time after treatment. Protein synthesis was dramatically inhibited, dropping to 31% of control cells after an 18 h treatment. The effect of the patellazoles on protein synthesis is further illustrated in a DNA microarray experiment. Of the 74 genes observed to be increasingly transcribed after treatment, 12 encode ribosomal proteins.

One pathway that plays a major role in regulating transcription in mammalian cells is the p70/mTOR pathway. In response to extracellular stimuli, a phosphorylation cascade occurs that activates ribosomal transcription. The patellazoles are able to decrease the phosphorylation of several members of this pathway, although the primary cellular target is not known. The inhibition point appears to be either downstream of AKT or in a parallel pathway. Downstream proteins 4EBP1 and S6 kinase are both affected by patellazole treatment, as well as the central protein p70 S6 kinase.

Rapamycin is a large hydroxylated macrolide that exhibits similar effects upon the p70/mTOR pathway in HCT 116 cells. Interestingly, treatment of HCT wild-type cells with patellazole B results in increased transcription of the rapamycin binding partner FKBP1 to levels 4.4 times that of the vehicle-treated cells. However, HCT 116 cells are much more resistant to rapamycin than to the patellazoles. The IC_{50} of rapamycin growth inhibition is 10 μM, 100–10 000 times less cytotoxic than the patellazoles in the HCT 116 cell lines. Compared to the patellazoles, rapamycin more strongly inhibits the p70 pathway, but is not as cytotoxic, implying differing targets or mechanisms of action. Another difference is that rapamycin-induced G_1 phase cell cycle arrest is mediated by a reduction is cyclin D1 [14], while treatment with the patellazoles does not affect the level of cyclin D1 (data not shown).

The target and mechanism of rapamycin was first described in yeast. Surprisingly, patellazole C is not able to inhibit the growth of yeast strains W303 and S288C (data not shown). Possible mechanisms of resistance include the exclusion of patellazole C by the yeast cell wall, increased metabolism of patellazole C or the mammalian target not being conserved in yeast. If, like rapamycin, the patellazoles do inhibit mTOR then further investigation into the nature of the yeast–patellazole interaction may provide clues to the mammalian mechanism of action.

The patellazoles continue to be both chemically and biologically interesting. Further chemical studies could include the elucidation of a crystal structure, which would provide both the stereochemistry of the 16 chiral carbons and information regarding global patellazole conformation. This information would be crucial in developing a synthetic route to the patellazoles, which would allow both more extensive biological testing and a potentially better method for accomplishing affinity chromatography or photoaffinity labeling. Selective labeling of the patellazole epoxide for use in such experiments has been unsuccessful so far. A synthetic scheme would also allow a library of patellazole-derived compounds to be synthesized for use in determining structure–activity relationships for the patellazoles and their cellular target or targets.

Acknowledgments

The authors would like to thank Dr Bert Vogelstein of Johns Hopkins University for generously donating the HCT 116 cell lines used in the majority of the cell-based experiments, and Robyn James and Mary Kay Harper for reviewing and editing this document. The flow cytometry and DNA microarray experiments were performed by the University of Utah Flow Cytometry Resource Facility and the Microarray Core Facility at the Huntsman Cancer Institute, respectively. Thanks are also given to the government of the Republic of the Fiji Islands and in particular the people of Kadavu Island and Nadroga Province for permission to collect marine organisms.

References

1 Zabriskie TM, Mayne CL, Ireland CM. Patellazole C. A novel cytotoxic macrolide from *Lissoclinum patella*. *J Am Chem Soc* 1988; **110**: 7919–7920.
2 Corley D, Moore R, Paul V. Patellazole B. A novel cytotoxic thiazole-containing macrolide from the marine tunicate *Lissoclinum patella*. *J Am Chem Soc* 1988; **110**:7920–7922.
3 Zabriskie TM. The characterization of cytotoxic metabolites from Fijian marine invertebrates. *Dissertation*. University of Utah, Salt Lake City; 1989.
4 Richardson AD. Chemical and biological studies of secondary metabolites from *Lissoclinum patella*. *Dissertation*. University of Utah, Salt Lake City; 2003.
5 Bio-Rad. *DC Protein Assay Instruction Manual*. Hercules, CA: Bio-Rad; 1997.
6 Life Technologies. *SDS–Polyacrylamide Gel System Form No. 18057P*. Carlsbad, CA: Life Technologies; 2000.
7 Schena M, Shalon D, Davis RW, Brown PO. Quantitative monitoring of gene expression patterns with a complementary DNA microarray. *Science* 1995; **270**:467–470.
8 Schena M, Shalon D, Heller R, Chai A, Brown PO, Davis RW. Parallel human genome analysis: microarray-based expression monitoring of 1000 genes. *Proc Natl Acad Sci USA* 1996; **93**:10614–10619.
9 Life Technologies. *Form No. 3820*. Carlsbad: CA: Life Technologies; 1999.
10 Promega. *Technical Manual TM021*. Madison, WI: Promega; 2000.
11 Mosmann T. Rapid colorimetric assay for cellular growth and survival: application to proliferation and cytotoxicity assays. *J Immunol Methods* 1983; **65**:55–63.
12 Kaufmann SH, Desnoyers S, Ottaviano Y, Davidson NE, Poirier GG. Specific proteolytic cleavage of poly(ADP-ribose) polymerase: an early marker of chemotherapy-induced apoptosis. *Cancer Res* 1993; **53**: 3976–3985.
13 Richardson AD, Ireland CM. A profile of the *in vitro* antitumor activity of lissoclinolide. *Toxicol Appl Pharmacol* 2004; **195**:55–61.
14 Hidalgo M, Rowinsky E. The rapamycin-sensitive signal transduction pathway as a target for cancer therapy. *Oncogene* 2000; **19**:6680–6686.
15 Weng QP, Kozlowski M, Belham C, Zhang A, Comb MJ, Avruch J. Regulation of the p70 S6 kinase by phosphorylation *in vivo*: analysis using site-specific anti-phosphopeptide antibodies. *J Biol Chem* 1998; **273**:16621–16629.

Copyright © Lippincott Williams & Wilkins. Unauthorized reproduction of this article is prohibited.